

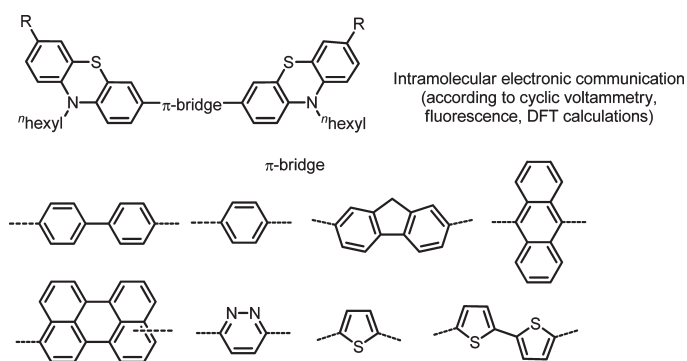
Luminescent, Redox-Active Diphenothiazine Dumbbells Expanded by Conjugated Arenes and Heteroarenes[‡]

Martina Hauck,[†] Raluca Turdean,^{†,‡} Karin Memminger,^{†,§} Jan Schönhaber,[†]
Frank Rominger,^{§,||} and T. J. J. Müller^{*,†}

[†]Institut für Organische Chemie und Makromolekulare Chemie, Heinrich-Heine Universität Düsseldorf, Universitätstrasse 1, D-40225 Düsseldorf, Germany, [‡]Babes-Bolyai University Cluj-Napoca, Faculty of Chemistry and Chemical Engineering, Arany Janos Str. No. 11, Cluj-Napoca 400428, Romania, and [§]Organisch-Chemisches Institut, Ruprecht-Karls-Universität Heidelberg, Im Neuenheimer Feld 270, D-69120 Heidelberg, Germany. ^{||}X-ray structure analysis.

thomasjj.mueller@uni-duesseldorf.de

Received October 8, 2010



Dumbbell-shaped diphenothiazines bridged by conjugatively linked (hetero)aromatic moieties were synthesized in a modular fashion by Suzuki–Miyaura coupling in good yields. The electronic structure was studied by DFT computations, determining the geometry optimized lowest energy conformers and scrutinizing the Kohn–Sham FMOs. The torsional deviation from coplanarity is predominantly influencing the electronic structure, i.e., by deviation from ideal overlap and maximal electron transmission. The reversible oxidation potentials assigned to the phenothiazinyl electrophores in most cases can thereby be qualitatively rationalized. All dumbbell-shaped diphenothiazines are strongly luminescent, which can be attributed to extended π -electron conjugation with considerable excited state electronic coupling as a consequence of large structural and electronic distributional changes upon photoexcitation.

Introduction

Functional organic molecules¹ are the key constituents for advanced molecule based electronics and photonics, and therefore the quest for new tailor-made and tunable functional molecules is an ongoing challenge to organic chemistry. Among many heteroaromatic systems, phenothiazines, their derivatives, and oligomers are highly interesting building blocks for rigid-rod and wire-like molecular modules for single-molecule electronics, as a consequence of their peculiar electronic

properties. In particular, their reversible formation of stable radical cations² and the tendency of alkynyl substituted and bridged phenothiazines³ to self-assemble on surfaces by π – π interactions⁴ or by thiol mediated chemisorptions⁵ renders them eligible as redox-switchable molecular entities in molecular materials and for functionalizing and redox-conditioning

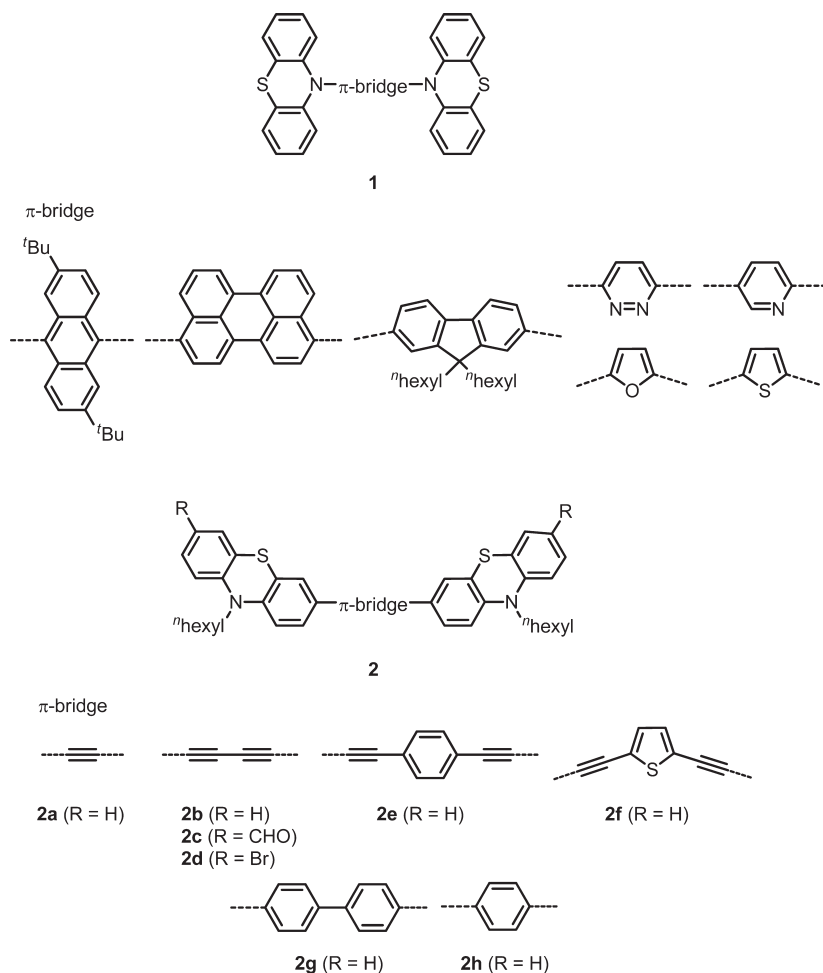
[‡] Dedicated to Prof. Dr. Dr. h. c. Franz Effenberger on the occasion of his 80th birthday.

(1) For a monograph, see: *Functional Organic Materials—Synthesis, Strategies, and Applications*, Müller, T. J. J., Bunz, U. H. F., Eds.; Wiley-VCH: Weinheim, 2007.

(2) (a) Oka, H. *J. Mater. Chem.* **2008**, *18*, 1927–1934. (b) Okamoto, T.; Kuratsu, M.; Kozaki, M.; Hirotsu, K.; Ichimura, A.; Matsushita, T.; Okada, K. *Org. Lett.* **2004**, *6*, 3493–3496. (c) Sun, D.; Rosokha, S. V.; Kochi, J. K. *J. Am. Chem. Soc.* **2004**, *126*, 1388–1401. (d) Kochi, J. K.; Rathore, R.; Le Maguères, P. *J. Org. Chem.* **2000**, *65*, 6826–6836. (e) Nishinaga, T.; Inoue, R.; Matsuura, A.; Komatsu, K. *Org. Lett.* **2002**, *4*, 1435–1438. (f) Pan, D.; Philips, D. L. *J. Phys. Chem. A* **1999**, *103*, 4737–4743.

(3) (a) Müller, T. J. J. *Tetrahedron Lett.* **1999**, *40*, 6563–6566. (b) Krämer, C. S.; Zeitler, K.; Müller, T. J. J. *Org. Lett.* **2000**, *2*, 3723–3726.

(4) Barkschat, C. S.; Guckenberger, R.; Müller, T. J. J. *Naturforsch.* **2009**, *64b*, 707–718.

CHART 1. Diphenothiazine Dumbbells with π -Conjugated N- and C-Bridges

of conductive surfaces. In particular, the transformation of phenothiazines into stable planar radical cations with excellent delocalization⁶ qualifies them as outstanding models for switchable conductive or semiconductive molecular wires with hole-transport properties.⁷ In addition, the inherent folded butterfly conformation of phenothiazine in the electronic ground state,⁸ also affects the luminescence properties of phenothiazines with extended π -conjugated substitution patterns. In many cases we could show that these derivatives are redox tunable to a large extent and that they display large

Stokes shifts,⁹ underlining the peculiar electronic structure of the excited state. Particularly interesting are diphenothiazine dumbbells **1** and **2**, which are conjugatively connected via a π -electron bridge (Chart 1).

Recently, we have reported the peculiar ground and excited state electronic properties of diphenothiazine dumbbells **1** ligated to the π -electron bridge via the 10-nitrogen substituent.^{9c,f} Cyclic voltammetry clearly showed that symmetrical dumbbell-shaped phenothiazine dyads bridged with short heterocyclic entities displayed intense electronic coupling between the redox-active phenothiazine moieties.^{9f} Furthermore, in the case of pyridyl-bridged derivatives the luminescence can be controlled by pH change, giving reversibly switchable, redox-active biselectrophore systems. For the anthracenyl bridged diphenothiazine an intense electronic coupling of the phenothiazinyl units is detected upon oxidation, whereas for the perylene-bridged dumbbell this ground state electronic coupling is essentially absent.^{9c} Yet, the emission spectra of both dumbbells reveal significant redshifts of the shortest wavelength emission bands and substantially larger Stokes shifts in comparison to anthracene or perylene.

A couple of years ago, we also reported on the ground and excited state electronic properties of diphenothiazine dumbbells **2a–f** ligated via alkynyl bridges at the 3-position of the phenothiazinyl benzo core.^{3,9a} Alkynyl bridging effected a

(5) (a) Franz, A. W.; Stoycheva, S.; Himmelhaus, M.; Müller, T. J. J. *Beilstein J. Org. Chem.* **2010**, *6*, published July 2, 2010; DOI:10.3762/bjoc.6.72. (b) Barkschat, C. S.; Stoycheva, S.; Himmelhaus, M.; Müller, T. J. J. *Chem. Mater.* **2010**, *22*, 52–63. (c) Lambert, C.; Kriegisch, V. *Langmuir* **2006**, *22*, 8807–8812.

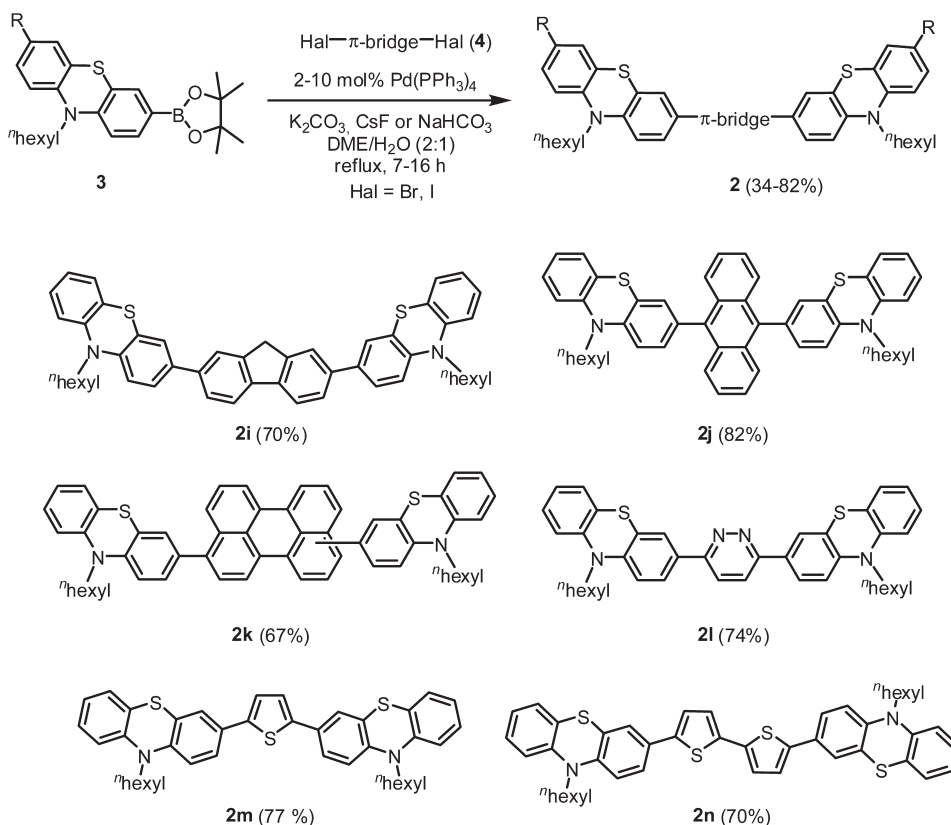
(6) Uchida, T.; Ito, M.; Kozawa, K. *Bull. Chem. Soc. Jpn.* **1983**, *56*, 577–582.

(7) Müller, T. J. J.; Franz, A. W.; Barkschat (née Krämer), C. S.; Sailer, M.; Meerholz, K.; Müller, D.; Colsmann, A.; Lemmer, U. *Macromol. Symp.* **2010**, *287*, 1–7.

(8) McDowell, J. J. H. *Acta Crystallogr., Sect. B: Found. Crystallogr.* **1976**, *B32*, 5–10.

(9) (a) Krämer, C. S.; Müller, T. J. J. *Eur. J. Org. Chem.* **2003**, 3534–3548.

(b) Sailer, M.; Nonnenmacher, M.; Oeser, T.; Müller, T. J. J. *Eur. J. Org. Chem.* **2006**, 423–435. (c) Franz, A. W.; F. Rominger, F.; Müller, T. J. J. *J. Org. Chem.* **2008**, *73*, 1795–1802. (d) Sailer, M.; Franz, A. W.; Müller, T. J. J. *Chem.–Eur. J.* **2008**, *14*, 2602–2614. (e) Franz, A. W.; Popa, L. N.; Müller, T. J. J. *Tetrahedron Lett.* **2008**, *49*, 3300–3303. (f) Franz, A. W.; Popa, L. N.; Rominger, F.; Müller, T. J. J. *Org. Biomol. Chem.* **2009**, *7*, 469–475.

SCHEME 1. Synthesis of Dumbbell-Shaped Diphenothiazinyl Triads **2i–n** Bridged by Different Aromatic and Heteroaromatic Spacers

weak electronic communication in the ground state by distance-dependent separation of the first oxidation potentials.³ As an indication of intensive intramolecular excited state communication red-shifted emission maxima, large Stokes shifts and substantial quantum yields have been measured by fluorescence spectroscopy. Phenylene and biphenylene bridged dumbbells **2g** and **2h** have been synthesized for establishing general synthetic accesses to substituted phenothiazines;¹⁰ however, the electronic properties have not been studied so far. Therefore, the peculiar electronic communication in N-bridged dumbbells **1** prompted us to scrutinize C-substituted dumbbells **2** with sp²-hybridized bridges in more detail. Here, we report the synthesis and electronic properties of diphenothiazine dumbbells expanded by conjugated arene and heteroarene bridges ligated to the core position 3.

Results and Discussion

Synthesis. Whereas N-ligated aromatic and heteroaromatic bridges in phenothiazine dumbbells **1**^{9c,f} were readily established by Buchwald–Hartwig N-arylation,¹¹ C-ligation is most efficiently achieved by Suzuki–Miyaura coupling¹²

with brominated or borylated phenothiazine precursors, a route that has been transposed and developed over the years in our laboratories.^{9b,d,e,10,13} Therefore, starting from the easily accessible 10-hexyl-10H-phenothiazin-3-yl pinacol boronic ester (**3**) (R = H),^{9d,13c} Suzuki–Miyaura coupling with a variety of dibromides or diiodides **4** gives rise to the formation of the dumbbell-shaped diphenothiazinyl triads **2i–n** as yellow to orange powders in good yields (Scheme 1). Since dibromoperylene **4c**, synthesized according to a literature procedure by Müllen et al.,¹⁴ was submitted as an inseparable mixture of the 3,9- and 3,10-dibromoperylene isomers, the dumbbell **2k** was expectedly obtained as a mixture of the 3,9- and 3,10-bridged isomers. The NMR spectra recorded in CD₂Cl₂ did not show two separate sets of signals. According to Müllen even the electronic properties of 3,9- and 3,10-substituted perylene isomers are almost identical, an important aspect for the subsequent discussion (*vide infra*).

For the synthesis of the 7-cyano substituted dumbbell **2o** the coupling protocol had to be inverted. As previously reported for the syntheses of the phenylene and biphenylene bridged dumbbells **2g** and **2h**,¹⁰ we decided to submit a

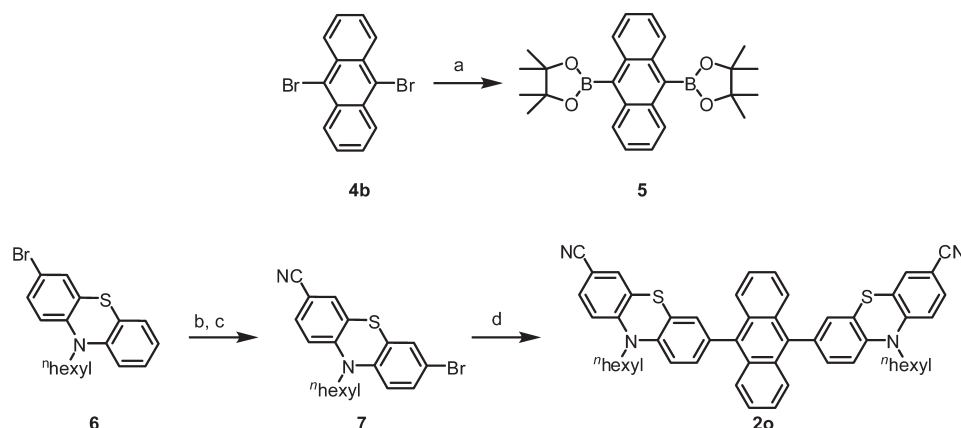
(10) Krämer, C. S.; Zeitler, K.; Müller, T. J. J. *Tetrahedron Lett.* **2001**, *42*, 8619–8624.

(11) (a) Guram, A. S.; Rennels, R. A.; Buchwald, S. L. *Angew. Chem., Int. Ed.* **1995**, *34*, 1348–1350. (b) Louie, J.; Hartwig, J. F. *Tetrahedron Lett.* **1995**, *36*, 3609–3612. (c) For reviews, see: Hartwig, J. F. In *Handbook of Organopalladium Chemistry for Organic Synthesis*; Negishi, E., Ed.; Wiley-Interscience: New York, 2002; pp 1051–1096. (d) Muci, A. R.; Buchwald, S. L. *Top. Curr. Chem.* **2002**, *219*, 131–209. (e) For an excellent overview of modern aromatic carbon-nitrogen cross-coupling reactions, see: Jiang, L.; Buchwald, S. L. In *Metal-Catalyzed Cross-Coupling Reactions*, 2nd ed.; De Meijere, A.; Diederich, F., Eds.; Wiley-VCH: New York, 2004; pp 699–760 and references therein.

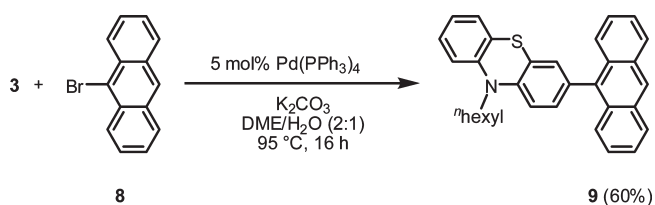
(12) (a) Miyaura, N.; Suzuki, A. *Chem. Rev.* **1995**, *95*, 2457–2483. (b) Suzuki, A. In *Metal Catalyzed Cross Coupling Reactions*; Stang, P. J.; Diederich, F., Eds.; Wiley-VCH: Weinheim, 1998; pp 49–97. (c) Stanforth, S. P. *Tetrahedron* **1998**, *54*, 263–303. (d) Suzuki, A. *J. Organomet. Chem.* **1999**, *576*, 147–168.

(13) (a) Franz, A. W.; Müller, T. J. J. *Synthesis* **2008**, 1121–1125. (b) Muschelknautz, C.; Sailer, M.; Müller, T. J. J. *Synlett* **2008**, 845–848. (c) Sailer, M.; Rominger, F.; Müller, T. J. J. *J. Organomet. Chem.* **2006**, *691*, 299–308. (d) Sailer, M.; Gropeanu, R.-A.; Müller, T. J. J. *J. Org. Chem.* **2003**, *68*, 7509–7512. (e) Krämer, C. S.; Zimmermann, T. J.; Sailer, M.; Müller, T. J. J. *Synthesis* **2002**, 1163–1170.

(14) Schlichting, P.; Rohr, U.; Müllen, K. *Liebigs Ann./Recueil* **1997**, 395–407.

SCHEME 2. Synthesis of Dumbbell-Shaped Nitrile-Substituted Anthracene-Bridged Phenothiazinyl Triad **2o**^a

^aReagents and conditions: (a) pinBBpin, KOAc, cat. Pd(OAc)₂, DMF, 77 °C, 8 h (60%). (b) K₄[Fe(CN)₆], NMP, cat. Pd(OAc)₂, cat. dppf, Na₂CO₃, 135 °C, 16 h (79%). (c) Br₂, CH₃CO₂H, rt, 16 h (81%). (d) **5**, cat. Pd(PPh₃)₄, K₂CO₃, DME/H₂O (2:1), 95 °C, 16 h (51%).

SCHEME 3. Synthesis of the 3-Anthracen-9-yl Phenothiazine Dyad **9**

bisborylated anthracene derivative to the coupling with the suitable 3-bromo-7-cyano phenothiazine derivative. The 9,10-bisborylated anthracene derivative **5** was prepared by Miyaura coupling from 9,10-dibromoanthracene (**4b**) with bis(pinacolato)diboron in good yield (Scheme 2).¹⁵ The required 3-bromo-7-cyano phenothiazine derivative **7** was synthesized in good yield via a two-step sequence starting with the Pd-catalyzed Beller cyanation^{16,9c} of 3-bromo-10-hexyl-10*H*-phenothiazine (**6**) and subsequent bromination with bromine in acetic acid at room temperature. Finally, the dumbbell-shaped triad **2o** was obtained by Suzuki–Miyaura coupling of the 3-bromo-7-cyano phenothiazine derivative **7** and the 9,10-bisborylated anthracene derivative **5** in good yield. Since 9-substitution of anthracenes implies considerable *peri*-interactions with torsional repulsion, we additionally prepared the 3-anthracen-9-yl phenothiazine derivative **9** as a reference compound by Suzuki–Miyaura coupling of the pinacolyl 10-hexyl-10*H*-phenothiazin-3-yl boronate (**3**) and the 9-bromo anthracene (**8**) in good yield (Scheme 3).

All structures were unambiguously assigned by ¹H and ¹³C NMR, UV–vis, and IR spectroscopy, mass spectrometry, and combustion analyses. The NMR spectra clearly support the highly symmetrical structure of all representatives **2** by

the appearance of the half set of resonances with respect to the actual number of nuclei. In addition for the dumbbell-shaped dithienyl bridged triad **2n** the structure was corroborated by an X-ray crystal structure analysis (Figure 1).¹⁷ Whereas the bithiophene unit in compound **2n** is planar a dihedral angle between the adjacent phenothiazinyl benzo-core and the bithienyl moiety accounts for a torsion by 30°. An inspection of the crystal packing shows that π -contacts between individual molecules in the crystal lattice are negligible, in particular, because the bridging bithiophenes do not π -stack. Therefore, electronic solid state interactions should be, if at all, relatively small.

Electronic Structure. The electronic structure of the dumbbell-shaped diphenothiazinyl triads **2** was first considered by computations on the DFT level of theory applying the B3LYP functional¹⁸ together with Pople's 6-311G(d,p) basis set¹⁹ as implemented in the program Gaussian03.²⁰ For saving computational time the *N*-hexyl substituents of the compounds **2** were truncated to *N*-ethyl substituents for the computations. Furthermore the minima structures were confirmed by analytical frequency analysis.

The structures of triads **2g–o** were geometry optimized upon imposing symmetry constraints (*C*₂-symmetry for the structures of **2g**, **2h**, **2k**,²¹ **2l**, **2m**; *C*_s-symmetry for the structures of **2i**, **2j**, **2o**; *C*₇-symmetry for the structure of **2n**). The computed torsional angles θ between the ligated phenothiazinyl benzo cores at the termini of the dumbbells and the π -conjugated bridges indicate a strong dependence of the torsion out of coplanarity from steric factors (Table 1). The orbital overlap of two adjacent π -systems, which is responsible for delocalization and transmission of electron density between the constituting moieties, correlates according to theory with $\cos \theta$, and the electron transmission with $\cos^2 \theta$.²² Hence, as a consequence of the steric biases of π -bridges

(15) (a) Yang, C.; Jacob, J.; Müllen, K. *Macromolecules* **2006**, *39*, 5696–5704. (b) Zhu, Y.; Rabindranath, A. R.; Beyerlein, T.; Tieke, B. *Macromolecules* **2007**, 6981–6989.

(16) Schareina, T.; Zapf, A.; Beller, M. *Chem. Commun.* **2004**, 1388–1389.

(17) Crystallographic data (excluding structure factors) for the structure reported in this paper have been deposited with the Cambridge Crystallographic Data Centre as supplementary publication no. CCDC 795807 (**2n**). Copies of the data can be obtained free of charge on application to CCDC, 12 Union Road, Cambridge CB2 1EZ, U.K. (Fax: + 44–1223/336–033. E-mail: deposit@ccdc.cam.ac.uk).

(18) (a) Becke, A. D. *J. Chem. Phys.* **1993**, *98*, 5648–5652. (b) Becke, A. D. *J. Chem. Phys.* **1993**, *98*, 1372–1377. (c) Parr, R. G.; Yang, W. *Density-Functional Theory of Atoms and Molecules*; Oxford University Press: Oxford, 1989.

(19) Ditchfield, R.; Hehre, W. J.; Pople, J. A. *J. Chem. Phys.* **1971**, *54*, 724–728.

(20) Frisch, M. J. et al. *Gaussian 03, Revision B.03*; Gaussian, Inc.: Wallingford, CT, 2004.

(21) Calculated for the 3,10-bridged isomer.

(22) Weitellier, S.; Launay, J. P.; Joachim, C. *Chem. Phys.* **1989**, *131*, 481–488.

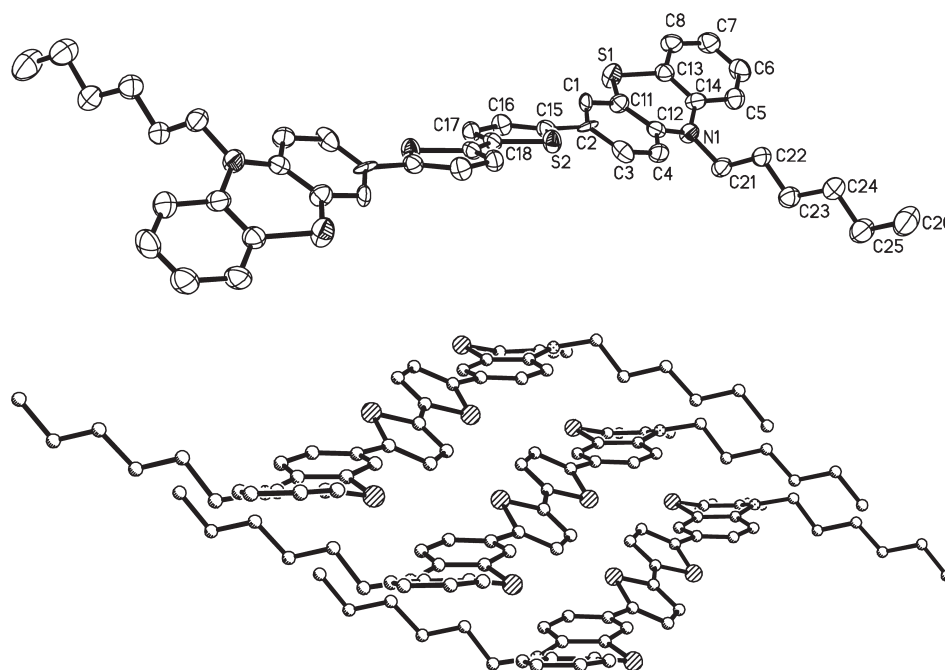


FIGURE 1. (Top) ORTEP plot of compound **2n** (hydrogen atoms are omitted for clarity). (Bottom) Coplanar orientation of the bithiophene bridges in the crystal lattice (hydrogen atoms are omitted for clarity).

TABLE 1. Selected Computed Torsional Angles of Diphenothiazine Dumbbells **2** and Orbital Overlap between Phenothiazines and Bridge

computed structure	torsional angles [deg]		orbital overlap [cos θ]	electron transmission [cos ² θ]
	$\theta_{\text{phenothiazine bridge}}$	$\theta_{\text{inner bridge}}$		
2g	37.95		0.79	0.62
2h	36.00	37.26	0.64 ^a	0.41 ^b
2i	38.69		0.78	0.61
2j	85.24		0.08	0.01
2k	55.50		0.57	0.32
2l	12.72		0.98	0.95
2m	29.64		0.87	0.75
2n	29.63	0	0.87 ^a	0.76 ^b
2o	86.42		0.06	0.00

^acos $\theta_{\text{phenothiazine bridge}}$ · cos $\theta_{\text{inner bridge}}$. ^bcos² $\theta_{\text{phenothiazine bridge}}$ · cos² $\theta_{\text{inner bridge}}$.

as such in 9,10-anthracenylene (structures **2j** and **2o**), the orbital overlap and the electronic transmission are considerably reduced, whereas 2,5-thienylene (structures **2m** and **2n**) and 3,6-pyridazinylene (structure **2l**) bridged systems essentially remain conjugated. With respect to the intramolecular electronic communication of the terminal phenothiazine electrophores in the ground state these aspects are of fundamental importance (*vide infra*).

For further discussion the energies (Figure 2) and the electron density distribution of the Kohn–Sham frontier orbitals (HOMO-2, HOMO-1, HOMO, LUMO, LUMO+1, LUMO+2; for figures, see Supporting Information) were taken into account. As a consequence of the imposed symmetry constraints in some cases degeneracy of the FMOs or at least relatively close gaps between the highest occupied FMOs is observed. Since the HOMO and the LUMO are of utmost importance for the discussion of the electronic properties (*vide infra*), a direct comparison of the FMOs of the computed structures **2** reveals some interesting features, which are again associated with the torsional biases of the

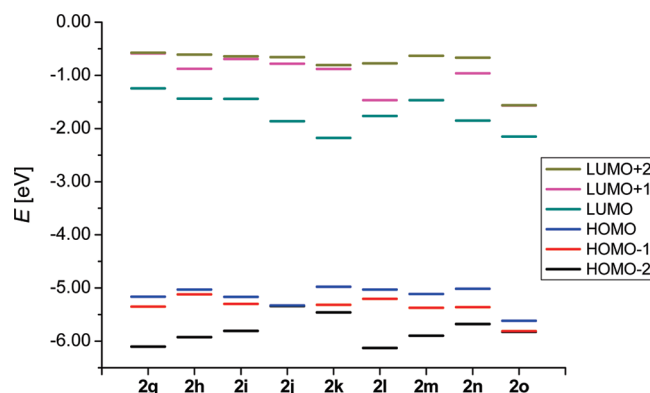


FIGURE 2. FMO energies (HOMO-2, HOMO-1, HOMO, LUMO, LUMO+1, LUMO+2) of the diphenothiazine dumbbells **2** (computed by DFT calculations with the B3LYP functional together with a 6-311G(d,p) basis set).

corresponding bridges (Figures 3 and 4). Already in the inspection of the electronic ground state it becomes apparent that the electron density distribution in the HOMOs is largely and equally allocated on the phenothiazinyl cores, but with two exceptions (Figure 3). Structure **2k** contains perylene as a bridge, which is an extended reasonably electron-rich π -system in its own right. Structure **2o** indicates, in contrary to the anthracenylene derivative structure **2j**, that the electron density distribution concentrates in the anthracene bridge. This latter finding can also be rationalized by the cyano substitution causing a diminished donor character of the phenothiazine unit. Interestingly, for the systems **2g**, **2i**, **2m**, and **2n** the coefficient distribution over the whole π -framework suggests a significant electronic interaction of the terminal phenothiazine moieties and the bridges. A similar behavior can be stated for the LUMOs, yet with a pronounced allocation of the electron density distribution on

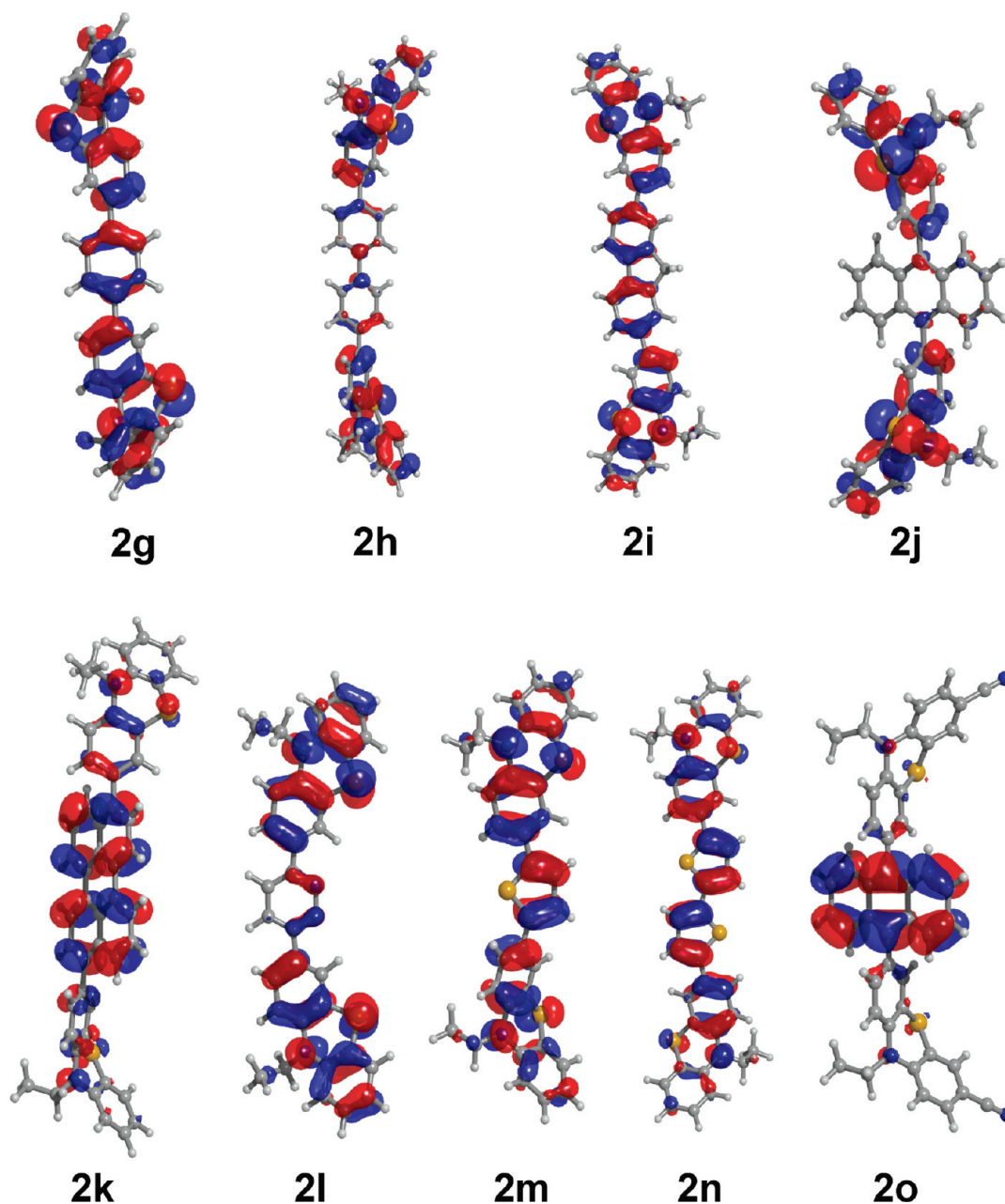


FIGURE 3. Kohn–Sham highest occupied molecular orbitals (HOMO) of the diphenothiazine dumbbells **2** (computed by DFT calculations with the B3LYP functional together with a 6-311G(d,p) basis set).

the bridging units (Figure 4). Expectedly, exclusive localization on the orthogonally oriented anthracene bridge is obtained for both systems **2o** and **2j**. The highly delocalized electron density distribution in the FMOs of all computed structures **2**, in particular, with considerable coefficient magnitudes on the bridging units, should impose significant effects in cyclic voltammetry and in the electronic spectra. Therefore, the experimentally determined electronic properties can be elucidated in the light of the computed features of the electronic structure.

Electronic Properties. Phenothiazine derivatives with extended π -conjugation are both redox-active and highly emissive functional π -electron systems.⁹ Therefore, the electronic properties of the dumbbell-shaped diphenothiazinyl triads **2** were scrutinized by studying ground state properties

by cyclic voltammetry and UV–vis absorption spectroscopy. Information about the excited state was collected by steady-state emission spectroscopy. Selected electronic properties of the phenothiazine dumbbells **2** and reference systems are summarized in Table 2.

Because all dumbbell-shaped diphenothiazinyl triads **2** are symmetrical (C_2 , C_s , or C_i point groups) and contain two phenothiazinyl units, the redox potentials in the anodic domain were studied by cyclic voltammetry. In addition, the electrochemical behavior also gives a clue to the electronic ground state structure, in particular, with respect to electronic communication of both electrophoric moieties. Upon comparison with the reference systems, such as *N*-hexyl-10*H*-phenothiazine, 3-cyano *N*-hexyl phenothiazine, anthracene, perylene, thiophene, and 2,2'-dithiophene, the

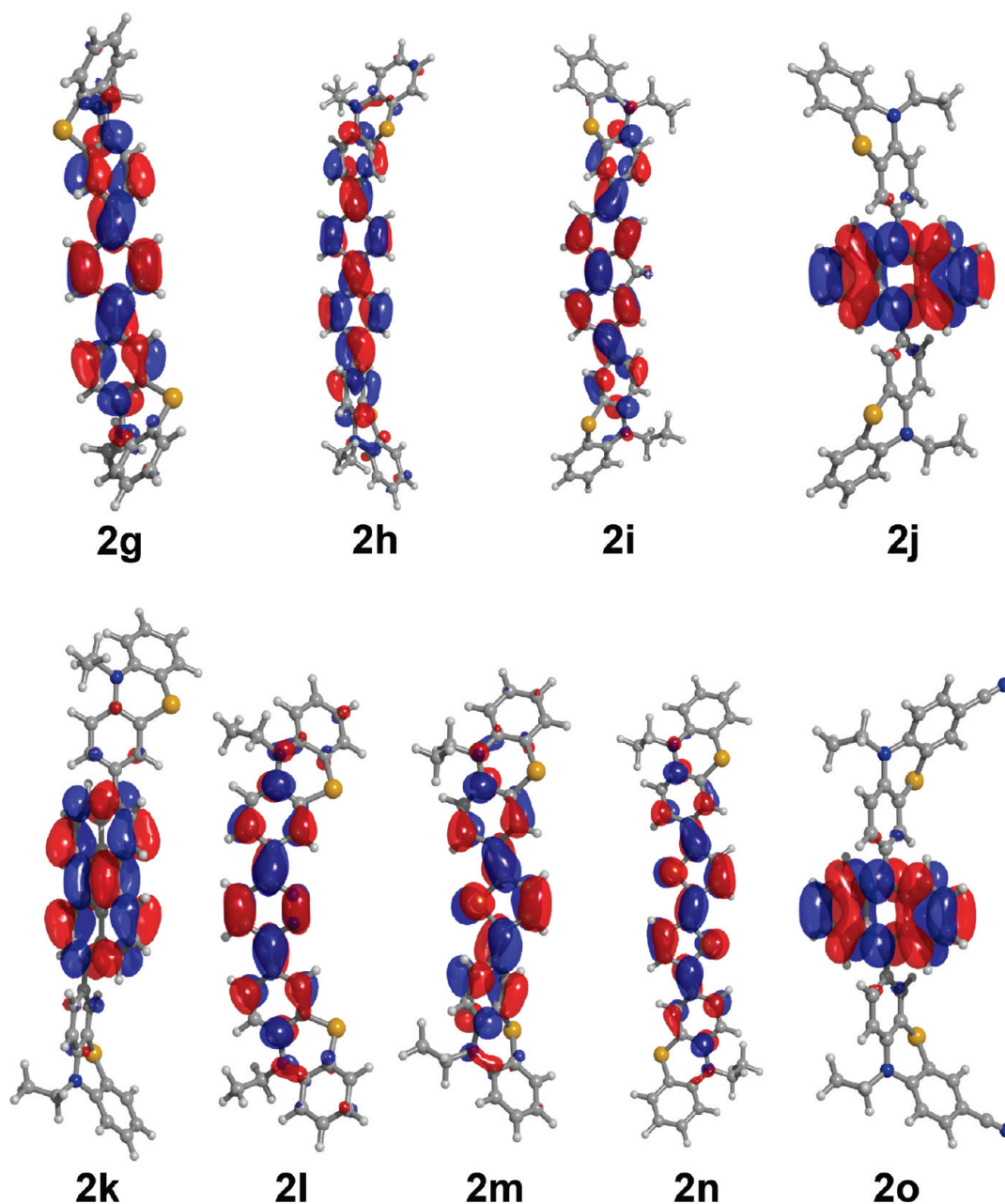


FIGURE 4. Kohn–Sham lowest unoccupied molecular orbitals (LUMO) of the diphenothiazine dumbbells **2** (computed by DFT calculations with the B3LYP functional together with a 6-311G(d,p) basis set).

first anodic oxidation potentials can be readily assigned to phenothiazine centered oxidations, but with the exception of the cyano substituted system **2o**.

Compounds **2j** and **2o** both share anthracene as a π -bridging moiety. Whereas the anthracene-phenothiazine dyad **9** clearly shows that the first oxidation occurs on the phenothiazinyl unit at a reversible one electron oxidation potential $E_0^{0/+1} = 738$ mV, almost identical with the potential $E_0^{0/+2} = 740$ mV for the triad **2j**, the first reversible oxidation of the cyano substituted system **2o** is considerably shifted anodically to appear at $E_0^{0/+1} = 974$ mV. Since the first reversible oxidation potential of 3-cyano *N*-hexyl phenothiazine appears cathodically shifted at $E_0^{0/+1} = 952$ mV, evidently the first oxidation of the cyano substituted system **2o** is caused rather by an anthracene centered oxidation. This interpretation

is not only supported by the oxidation potential of anthracene ($E_0^{0/+1} = 940$ mV) but also by the computed electronic structure. The HOMO of structure **2o**, which is predominantly relevant for the electrochemical oxidation, is allocated almost exclusively on the anthracene bridge (Figure 3). Therefore, in the cyano substituted anthracene bridged diphenothiazine dumbbell, the reversible oxidation occurs on the anthracene moiety and not at the phenothiazinyl termini.

Interestingly, a weak electronic communication in the title compounds can be identified by appearance of distinct shoulders only in the cyclic voltammogram in the cases of the *p*-phenylene (**2g**), the thien-2,5-diylene (**2m**), and the 2,2'-dithien-5,5'-diylene (**2n**) bridged dumbbells (Figure 5). Upon convolution of the cyclic voltammograms with a $1/\sqrt{t}$ function

TABLE 2. Selected Electronic Properties of Diphenothiazine Dumbbells **2** Bridged by Various Spacers, *N*-Hexyl-10*H*-phenothiazine, 3-Cyano *N*-Hexyl Phenothiazine, Anthracene, Perylene, Thiophene, and 2,2'-Dithiophene (Cyclic Voltammetry,^a Absorption,^b and Emission^b Spectra)

compound	$E_0^{0/+1}$ [mV]	$E_0^{+1/+2}$ [mV]	absorption $\lambda_{\max, \text{abs}}$ [nm]	emission $\lambda_{\max, \text{em}}$ [nm]	Stokes shift $\Delta \tilde{\nu}$ [cm ⁻¹]	quantum yield Φ_f
<i>N</i> -hexyl phenothiazine ²³	728		258, 312			
3-phenyl <i>N</i> -hexyl phenothiazine ^{9b}	701		268, 322	456	9100	0.10 ^c
3-cyano <i>N</i> -hexyl phenothiazine ^{9c}	952		268, 340	474, 491sh	8300	0.11 ^d
anthracene ²⁴	940		312, 323, 339, 356, 376 ^e	376, 397, 420, 446, 475, 508 ^e	0	0.32 ^e
perylene ²⁵	940	1640	253, 386, 408, 436 ^e	436, 463, 496, 528, 594 ^e	0	0.94 ^e
thiophene ^{26,27}	> 1800 ^{f,g}		243			
2,2'-dithiophene ^{26,28}	1460		248, 304 ^h	366 ^g	5600	0.01 ⁱ
2g ¹⁰	700	736	240, 271, 287, 345sh	471	7500	0.27 ^c
2h ¹⁰	705 ^j		242, 269, 306, 351sh	477	8400	0.36 ^c
2i	678 ^j		262, 329, 362	488	7200	0.60 ^d
2j	740 ^j		258, 315, 359, 379, 398	572	7600	0.01 ^k
2k	707 ^j	1080 ^l	259, 316, 441, 468	579	4100	0.36 ^k
2l	764 ^j		278, 299, 394	521	6200	0.34 ^d
2m	649	758	245, 258, 321, 390	493	5300	0.17 ^c
2n	651	713	250, 266, 338, 418	520	4700	0.08 ^c
2o	974		259, 266, 327, 341, 360, 379, 398	509	5500	0.14 ^k
9	738	1342	255, 317, 332, 350, 368, 388	440	3000	0.04 ^m

^aRecorded in CH₂Cl₂, 20 °C, electrolyte = "Bu₄⁺PF₆⁻, Pt working electrode, Pt counter electrode, Ag/AgCl reference electrode. ^bRecorded in CH₂Cl₂. ^cDetermined in CH₂Cl₂ with perylene as a standard ($\Phi_f = 0.94$). ^dDetermined in CH₂Cl₂ with coumarin 151 in ethanol as a standard ($\Phi_f = 0.49$). ^eRecorded in cyclohexane. ^fRecorded in benzonitrile, 20 °C, electrolyte = "Bu₄⁺ClO₄⁻, Pt working electrode, Pt counter electrode, Ag/AgCl reference electrode. ^gPolymerization upon oxidation. ^hRecorded in THF. ⁱDetermined in THF with quinine sulfate as a standard ($\Phi_f = 0.54$). ^j $E_0^{0/+2}$ was detected. ^kDetermined in CH₂Cl₂ with coumarin 153 in ethanol as a standard ($\Phi_f = 0.38$). ^l $E_0^{+2/+3}$ was detected. ^mDetermined in CH₂Cl₂ with 9,10-diphenylanthracene in cyclohexane as a standard ($\Phi_f = 0.90$).

the separated oxidation potentials can be extracted. The peak separations and hence the intramolecular coupling of the stepwise oxidation diminish from the 2,5-thienylene ($\Delta E = 109$ mV) over the dithienylene ($\Delta E = 62$ mV) to the *p*-phenylene bridge ($\Delta E = 36$ mV). This behavior can be rationalized by the increased diaryl torsion of the phenylene unit in comparison to the thienyl bridge (*vide supra*). Increasing the intramolecular distance of the electrophores (thienylene vs dithienylene) expectedly reduces the electronic coupling and for the 4,4'-biphenylene bridge (**2h**) coupling is already undetectable in the cyclic voltammetry experiment as shown by the appearance of only one simultaneous fully reversible Nernstian oxidation potential $E_0^{0/+2}$ for both phenothiazine moieties.

The same behavior holds true for the dumbbell-shaped diphenothiazinyl triads **2i**–**2l** (Figure 6). With the exception of triad **2o** ($E_0^{0/+1} = 974$ mV), which only displays a one electron oxidation, the reversible oxidation potentials are found in a relatively narrow range from $E_0^{0/+2} = 678$ to 764 mV. Attempts to correlate the first oxidation potentials to computed HOMO energies, as previously established for (hetero)aryl ethynyl *N*-methyl phenothiazines^{9a} or consanguinous series of 3-(hetero)aryl-substituted and 3,7-di(hetero)aryl-substituted *N*-hexyl phenothiazines,^{9b} were met with failure. However, this can be understood due to the complicated

interplay of steric and torsional effects of the bridging π -systems effective in the series of the title compounds **2g**–**o**.

Interestingly, the perylene bridged system **2k** exhibits an additional one-electron oxidation at $E_0^{+2/+3} = 1080$ mV, which can be associated with an electron transfer from the perylene bridge. In comparison to perylene this potential is shifted anodically as a consequence of the adjacent positively charged phenothiazinyl radical ions.

Optical spectroscopy (UV–vis and fluorescence spectra) of dumbbell-shaped diphenothiazinyl triads **2** shows intense absorption bands in a range from 345 to 468 nm and blue to yellow luminescence with broad bands ranging from 471 to 579 nm (Table 2). As already found for many phenothiazinyl systems with extended π -conjugation⁹ again this class of luminescent, redox-active chromophores displays large Stokes shifts (4100–8400 cm⁻¹) with substantial emission efficiency, underlined by the quantum yields Φ_f in a range from 0.01 to 0.60.

A closer inspection of the absorption spectra, also in comparison to the spectra of the subunits as references, reveals that in all cases a substantial redshift of the longest wavelength absorption maxima is caused by increased π -electron conjugation. However, the extent of this overall bathochromic shift is largely determined by the torsionally affected overlap (*vide supra*). As a consequence the redshifts of the almost orthogonal anthracene bridged triads **2j** and **2o** ($\lambda_{\max, \text{abs}} = 398$ nm), and the dyad model **9** ($\lambda_{\max, \text{abs}} = 388$ nm) are relatively small in comparison to anthracene ($\lambda_{\max, \text{abs}} = 376$ nm) yet reproduce the vibrational fine structure of the anthracene derived *p*-band. In contrast, the slightly twisted thienyl systems **2m** and **2n** experience a pronounced increase in delocalization and hence in a reduced energy gap for the excitation ($\lambda_{\max, \text{abs}} = 390$ and 418 nm, respectively) in comparison to the constituents *N*-hexyl phenothiazine ($\lambda_{\max, \text{abs}} = 312$ nm), thiophene ($\lambda_{\max, \text{abs}} = 243$ nm), or 2,2'-dithiophene ($\lambda_{\max, \text{abs}} = 304$ nm). The same holds true for the pyridazinylene system **2l** ($\lambda_{\max, \text{abs}} = 394$ nm).

Also the phenylene (**2g**), biphenylene (**2h**), fluorenylene (**2i**), and perylene (**2k**) bridged systems with intermediate

(23) Clarke, D.; Gilbert, B. C.; Hanson, P.; Kirk, C. M. *J. Chem. Soc., Perkin Trans. 2* **1978**, 1103–1110.

(24) (a) Du, H.; Fuh, R. A.; Li, J.; Corkan, A.; Lindsey, J. S. *Photochem. Photobiol.* **1998**, *68*, 141–142. (b) Magdesieva, T. V.; Kukhareva, I. I.; Shaposhnikova, E. N.; Artamkina, G. A.; Beletskaya, I. P.; Butin, K. P. *J. Organomet. Chem.* **1996**, *526*, 51–58.

(25) (a) Fukuzumi, S.; Ohkubo, K.; Imahori, H.; Guldi, D. M. *Chem.—Eur. J.* **2003**, *9*, 1585–1593. (b) Donkers, R. L.; Maran, F.; Wayner, D. D. M.; Workentin, M. S. *J. Am. Chem. Soc.* **1999**, *121*, 7239–7248. (c) Dietrich, M.; Heinze, J. *J. Am. Chem. Soc.* **1990**, *112*, 5142–5145.

(26) Fichou, D.; Nunzi, J.-M.; Charra, F.; Pfeffer, N. *Mol. Cryst. Liq. Cryst. Sci. Technol., Sect. A* **1994**, *255*, 73–84.

(27) Inoue, S.; Jigami, T.; Nozoe, H.; Otsubo, T.; Ogura, F. *Tetrahedron Lett.* **1994**, *35*, 8009–8012.

(28) Ortiz, R. P.; Casado, J.; Hernández, V.; Navarrete, J. T. L.; Letizia, J. A.; Ratner, M. A.; Facchetti, A.; Marks, T. J. *Chem.—Eur. J.* **2009**, *15*, 5023–5039.

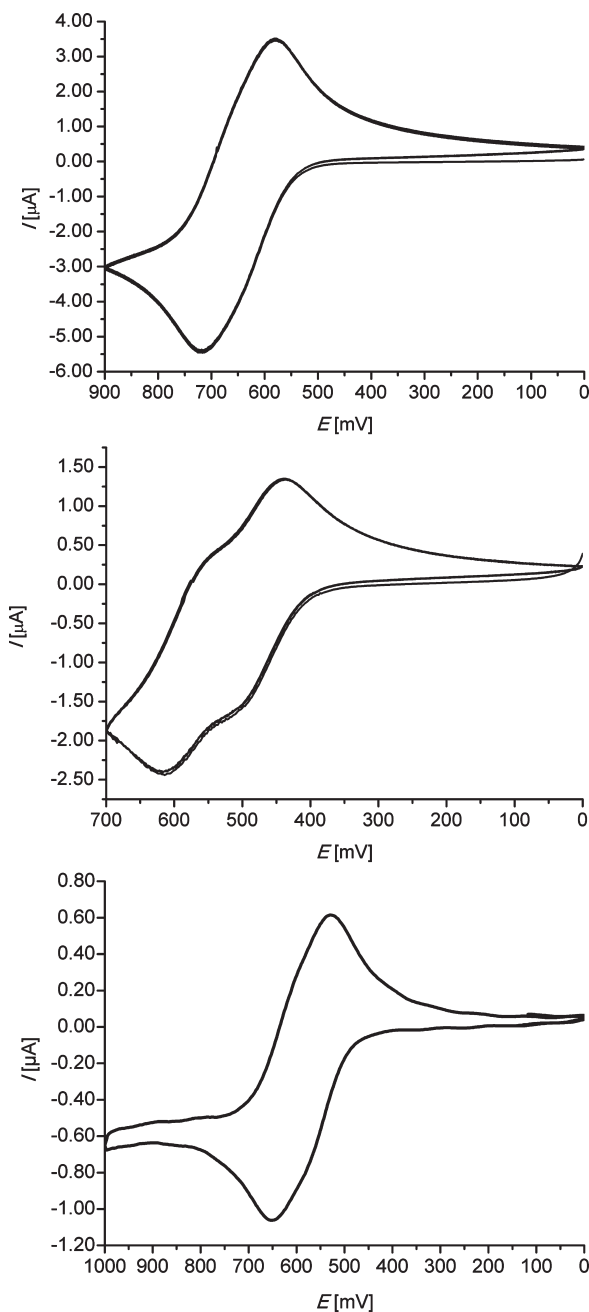


FIGURE 5. Cyclic voltammograms of **2g** (top), **2m** (center), and **2n** (bottom) (recorded in dichloromethane, $T = 293\text{ K}$, $v = 100\text{ mV/s}$, electrolyte = $n\text{Bu}_4\text{N}^+ \text{PF}_6^-$, Pt working electrode, Pt counter electrode, Ag/AgCl reference electrode).

torsional angles experience extended delocalization and, therefore, red-shifted longest wavelength absorption maxima.

A linear regression analysis reveals a moderate correlation of the computed HOMO–LUMO gap of the structure of **2** with the experimentally determined longest wavelength absorption maxima extracted from the UV–vis spectra ($r^2 = 0.82156$). Keeping in mind the contribution of several conformers to the actual spectra and the pronounced differences in torsional angles θ (*vide supra*), *cum grano salis* this correlation suggests that the longest wavelength absorption bands predominantly originate from HOMO–LUMO transitions. With respect to the discussed coefficient distribution in

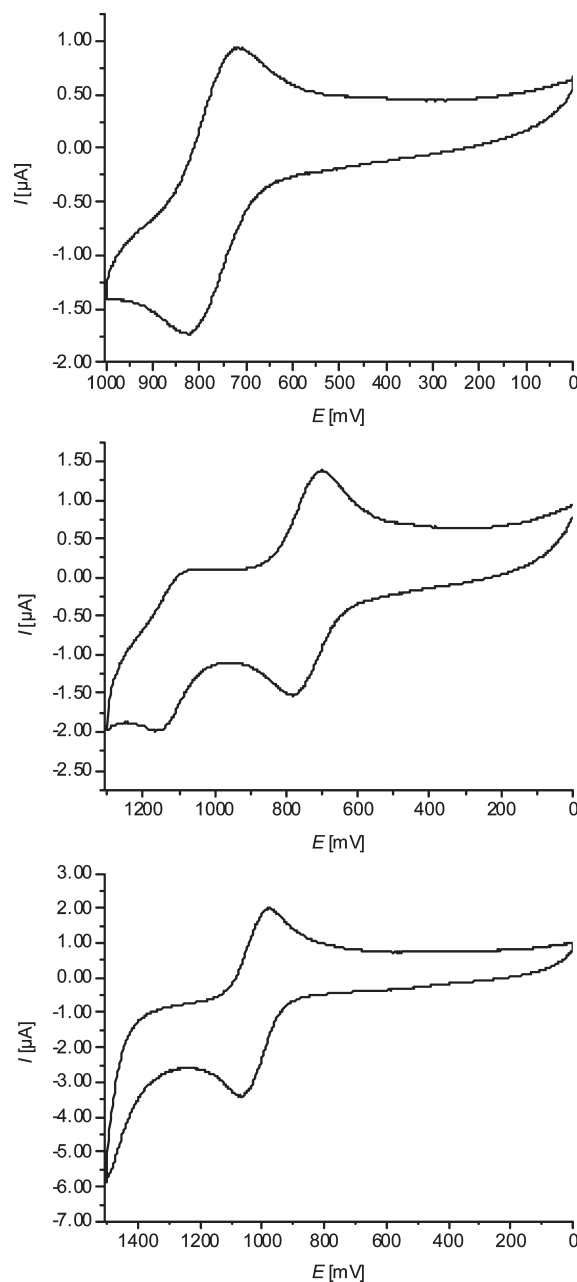


FIGURE 6. Cyclic voltammograms of **2j** (top), **2k** (center), and **2o** (bottom) (recorded in dichloromethane, $T = 293\text{ K}$, $v = 100\text{ mV/s}$, electrolyte = $n\text{Bu}_4\text{N}^+ \text{PF}_6^-$, Pt working electrode, Pt counter electrode, Ag/AgCl reference electrode).

the FMOs this rationale appears to be quite plausible and is additionally supported by relatively large extinction coefficients of these maxima indicating large oscillator strengths and substantial transition dipole moments.

Most interestingly, however, is the observed luminescence behavior of the investigated title compounds **2**. All systems reveal large Stokes shifts, which originate from large geometrical changes upon excitation from a highly nonplanar, ground state with a butterfly conformation to an essentially planarized excited state.²⁹ Hence, intense electronic communication of the

(29) Yang, L.; Feng, J.-K.; Ren, A.-M. *J. Org. Chem.* **2005**, *70*, 5987–5996.

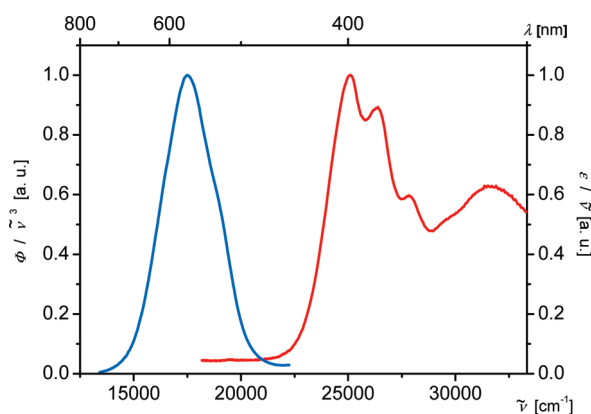


FIGURE 7. Normalized UV-vis (red line) and fluorescence (blue line) spectra of **2j** (recorded in dichloromethane, $T = 298$ K, UV-vis: $c(\mathbf{2j}) = 10^{-3}$ M; emission: $c(\mathbf{2j}) = 10^{-6}$ M; $\lambda_{\text{max,exc}} = 398 \pm 15$ nm).

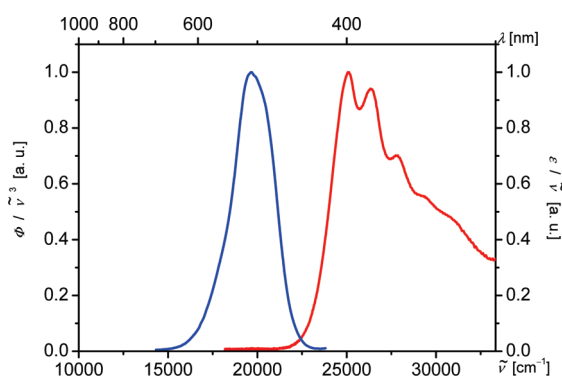


FIGURE 8. Normalized UV-vis (red line) and fluorescence (blue line) spectra of **2o** (recorded in dichloromethane, $T = 298$ K, UV-vis: $c(\mathbf{2o}) = 10^{-3}$ M; emission: $c(\mathbf{2o}) = 10^{-6}$ M; $\lambda_{\text{max,exc}} = 398 \pm 15$ nm).

π -system constituents should be enabled in the vibrationally relaxed excited state. A closer inspection of the emission spectra for the anthracenyl (**2j** and **2o**) and perylene (**2k**) bridged systems disclose intriguing features (Figures 7–9). First, the emission spectra represent neither phenothiazinyl nor bridge characteristic emission maxima but display considerably red-shifted, broad bands, i.e., large Stokes shifts. Whereas in the absorption spectra of the anthracenyl bridged dumbbells **2j** and **2o** the vibrational fine structure of the anthracene derived p -band can clearly be recognized, the expected mirror image fluorescence spectra are not found. Hence, the emission characteristics obviously result from significant structural changes and/or electronic redistribution, e.g., by charge transfer.³⁰ The former aspect is supported by excited state computations of oligophenothiazines suggesting planarization of the phenothiazinyl units.²⁹ The latter condition is in good agreement with the electronic structure of the HOMO and LUMO (Figures 3 and 4), where the longest wavelength absorption bands are dominated by charge transfer from the terminal phenothiazine moieties into the conjugated bridge. Therefore, it is very likely that the emission occurs from a relaxed excited state with considerable dipolar (for **9**) or quadrupolar (for **2**) charge transfer

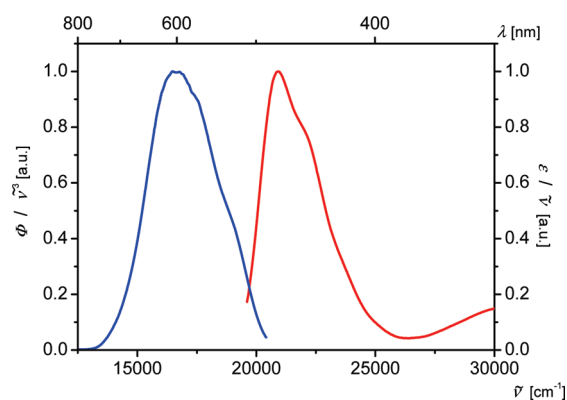


FIGURE 9. Normalized UV-vis (red line) and fluorescence (blue line) spectra of **2k** (recorded in dichloromethane, $T = 298$ K, UV-vis: $c(\mathbf{2k}) = 10^{-3}$ M; emission: $c(\mathbf{2k}) = 10^{-6}$ M; $\lambda_{\text{max,exc}} = 468 \pm 15$ nm).

character. Whereas the phenothiazines and anthracene are largely electronically decoupled in the electronic ground state of **2j**, **2o**, and **9**, the excited state electronic structure accounts for intense electronic coupling of the constituents. Second, the expanded π -system structure especially of only slightly twisted bridges manifests in new features, e.g., thiophene and pyridazine³¹ are essentially nonfluorescent, and N -hexyl phenothiazine and 2,2'-dithiophene only display a minimal, negligible emission at room temperature. In contrast, not only are the dumbbells **2l,m** emissive but also the fluorescence quantum yields Φ_f are multiply increased. Third, rigid bridges with pronounced emission characteristics and absent Stokes shifts, such as perylene ($\Phi_f = 0.94$) or anthracene ($\Phi_f = 0.32$), upon incorporation in the dumbbells display large Stokes shifts and diminished quantum yields (**2k**: $\Phi_f = 0.36$; **2j**: $\Phi_f = 0.01$; **2o**: $\Phi_f = 0.14$; **9**: $\Phi_f = 0.04$). As a consequence and in contrary to the electronically and sterically uniform diphenothiazine dumbbells **1**, all dumbbells **2** are characterized by unique emission properties and luminescence tunable by the nature, the conformational biases, and the rigidity of the bridging π -system. In addition, the occurrence of reversible redox behavior should be highly favorable for electrochemical switching of the luminescence.

Conclusion

In summary we could successfully synthesize dumbbell-shaped diphenothiazines bridged by conjugatively linked (hetero)aromatic moieties in a modular fashion by Suzuki–Miyaura coupling in good yields. The electronic structure was approached by DFT computations, determining the geometry optimized lowest energy conformers and scrutinizing the Kohn–Sham FMOs. Expectedly, the electronic structure is predominantly influenced by torsional deviation from coplanarity, i.e., from ideal overlap and maximal electron transmission. Against this background the reversible oxidation potentials resulting from the phenothiazinyl electrophores in most cases can be qualitatively rationalized. Furthermore, all dumbbell-shaped diphenothiazines are strongly luminescent and behave in good agreement with the computed electronic structure as systems with extended π -electron conjugation with considerable excited state electronic coupling as a consequence of large structural and

(30) (a) Valeur, B. *Molecular Fluorescence*; Wiley-VCH: Weinheim, 2002. (b) Lakowicz, J. R. *Principles of Fluorescence Spectroscopy*, 3rd ed.; Springer: New York, 2006.

(31) Li, H.; Dupre, P.; Kong, W. *Chem. Phys. Lett.* **1997**, *273*, 272–278.

electronic distributional changes upon photoexcitation. All this qualifies these symmetrical redox-active dumbbells as tunable and electrochemical switchable emissive components for future photonic or electronic applications. Further studies addressing the synthesis, the emission, and electrochemical characteristics of highly polarized and polarizable phenothiazine based lumophores are currently underway.

Experimental Section

General Considerations. Reagents, catalysts, ligands, and solvents were purchased as reagent grade and used without further purification. DME and DMF were dried and distilled according to standard procedures.³² 10-Hexyl-10*H*-phenothiazin-3-yl pinacolyl boronic ester (**3**),^{9d,13c} 3,9(3,10)-dibromoperylene (**4c**),¹⁴ 5,5'-diiido-[2,2']-bithiophene (**4f**),³³ 9,10-di(4,4,5,5-tetramethyl-1,3,2-dioxaborolan-2-yl)anthracene (**5**),¹⁵ and 3-bromo-10-hexyl-10*H*-phenothiazine (**6**)^{9d} were prepared according to literature procedures. Column chromatography: silica gel 60 mesh 230–400. TLC: silica gel plates. Melting points: uncorrected values. ¹H and ¹³C NMR spectra in CD₂Cl₂, acetone-*d*₆, or THF-*d*₈. The assignments of quaternary C, CH, CH₂, and CH₃ have been made by using DEPT spectra. The standards for determining the fluorescence quantum yields were perylene ($\Phi_f = 0.94$),³⁴ coumarin 151 ($\Phi_f = 0.49$),³⁵ quinine sulfate ($\Phi_f = 0.54$),³⁶ coumarin 153 ($\Phi_f = 0.54$),³⁷ and 9,10-diphenyl anthracene ($\Phi_f = 0.90$).³⁸

Electrochemistry. Cyclic voltammetry experiments were performed under argon in dry and degassed CH₂Cl₂ at room temperature and at scan rates of 100, 250, 500, and 1000 mV s⁻¹. The electrolyte was Bu₄NPF₆ (0.025 M). The working electrode was a 1 mm platinum disk, the counter-electrode was a platinum wire, and the reference electrode was an Ag/AgCl electrode. The potentials were corrected to the internal standard of Fc/Fc⁺ in CH₂Cl₂ ($E_0^{0/+1} = 450$ mV).³⁹

3-Bromo-7-cyano-10-hexyl-10*H*-phenothiazine (7). Bromine (5.18 mmol, 0.26 mL) is added dropwise to a solution of 3-cyano-10-hexyl-10*H*-phenothiazine^{9e} (4.71 mmol, 1.46 g) in 40 mL of glacial acetic acid. The reaction mixture is stirred at room temperature for 16 h. Then, dichloromethane (50 mL) and an oversaturated solution of Na₂SO₃ (50 mL) are added, and the mixture is stirred for another 30 min. The aqueous layer is extracted several times with small amounts of dichloromethane. The combined organic layers are dried with anhydrous sodium sulfate, and the solvent is removed *in vacuo*. The residue is chromatographed on silica (hexane to *n*-hexane/acetone 10:1) to give **7** (1.47 g, 81%) as a yellow solid, mp 69 °C. ¹H NMR (500 MHz, acetone-*d*₆): δ 0.84 (s, 3 H), 1.28 (m, 4 H), 1.44 (m, 2 H), 1.77 (m, 2 H), 3.98 (t, $J = 7.0$ Hz, 2 H), 7.02 (d, $J = 8.5$ Hz, 1 H), 7.15 (d, $J = 8.0$ Hz, 1 H), 7.30 (s, 1 H), 7.36 (d, $J = 8.5$ Hz, 1 H), 7.49 (s, 1 H), 7.57 (d, $J = 7.0$ Hz, 1 H). ¹³C NMR (125 MHz, acetone-*d*₆): δ 15.2 (CH₃), 24.2 (CH₂), 27.9 (CH₂), 28.1 (CH₂), 33.0 (CH₂), 49.2 (CH₂), 107.4 (C_{quat}), 117.1 (C_{quat}), 117.9 (CH), 119.8 (CH), 119.9 (CH), 126.4 (C_{quat}), 127.5 (C_{quat}), 131.2 (CH), 132.0 (CH), 132.4 (CH), 133.9 (CH), 145.0 (C_{quat}), 150.7 (C_{quat}). EI MS (70 eV, m/z (%)): 388 ([M⁺], 100), 301 ([M⁺ - C₆H₁₃], 50). UV-vis (CH₂Cl₂): λ_{\max} (ϵ) = 270 nm (123700), 328 nm

(17600). IR (KBr): $\tilde{\nu} = 2913$ cm⁻¹, 2221, 1596, 1496, 1460, 752. Anal. Calcd for C₁₉H₁₉BrN₂S (387.3): C 58.92, H 4.94, N 7.23. Found: C 58.89, H 4.96, N 7.18.

2,7-Bis(10-hexyl-10*H*-phenothiazin-3-yl)-9*H*-fluorene (2i). A mixture of 2,7-dibromo-9*H*-fluorene (**4a**) (0.21 mmol, 68 mg), 10-hexyl-10*H*-phenothiazin-3-yl pinacolyl boronic ester (**3**) (0.464 mmol, 190 mg), and cesium fluoride (2.10 mmol, 319 mg) in a mixture of 5 mL of dimethoxyethane and 2.5 mL of distilled water is degassed with nitrogen for 20 min, and then tetrakis(triphenylphosphine)palladium (21 μ mol, 24 mg) is added. The reaction is heated to reflux temperature for 8 h. After cooling to room temperature, dichloromethane, water, and an oversaturated solution of Na₂SO₃ are added. The aqueous layer is extracted several times with small amounts of dichloromethane. The combined organic layers are dried with anhydrous sodium sulfate, and the solvent is removed *in vacuo*. The residue is chromatographed on silica (*n*-hexane/acetone 10:1) to give **2i** (101 mg, 70%) as a yellow solid, mp 82–83 °C. ¹H NMR (500 MHz, THF-*d*₈): δ 0.86–0.88 (m, 6 H), 1.30–1.32 (m, 8 H), 1.46–1.49 (m, 4 H), 1.78–1.84 (m, 4 H), 3.92 (t, $J = 7.0$ Hz, 4 H), 3.97 (s, 4 H), 6.87 (t, $J = 7.5$ Hz, 2 H), 6.95 (d, $J = 8.5$ Hz, 2 H), 7.01 (d, $J = 8.0$ Hz, 2 H), 7.09–7.14 (m, 4 H), 7.45 (d, $J = 1.5$ Hz, 2 H), 7.48 (dd, $J = 7.5$ Hz, $J = 1.50$ Hz, 2 H), 7.59 (d, $J = 8$ Hz, 2 H), 7.78 (s, 2 H), 7.82 (d, $J = 8.0$ Hz, 2 H). ¹³C NMR (125 MHz, THF-*d*₈): δ 14.2 (CH₃), 23.4 (CH₂), 27.3 (CH₂), 27.6 (CH₂), 32.3 (CH₂), 37.5 (CH₂), 47.8 (CH₂), 116.2 (CH), 116.3 (CH), 120.7 (CH), 122.9 (CH), 123.5 (CH), 125.4 (C_{quat}), 125.8 (CH), 126.0 (CH), 126.2 (CH), 126.3 (C_{quat}), 127.86 (CH), 127.88 (CH), 136.4 (C_{quat}), 139.3 (C_{quat}), 141.1 (C_{quat}), 145.0 (C_{quat}), 145.3 (C_{quat}), 146.0 (C_{quat}). MALDI MS $m/z = 728.3$ (EM = 728.33). UV-vis λ_{\max} (ϵ) = 262 nm (38700), 329 nm (40100), 362 nm (40000). IR (KBr): $\tilde{\nu} = 2924$ cm⁻¹, 1637, 1602, 1577, 1542, 1508, 1491, 1467, 1442, 749. Anal. Calcd for C₄₉H₄₈N₂S₂ (729.1): C 80.72, H 6.64, N 3.84. Found: C 80.51, H 6.86, N 3.71.

9,10-Bis(10-hexyl-10*H*-phenothiazin-3-yl)anthracene (2j). A mixture of 9,10-dibromoanthracene (**4b**) (0.20 mmol, 67 mg), 10-hexyl-10*H*-phenothiazin-3-yl pinacolyl boronic ester (**3**) (0.44 mmol, 0.18 g), and potassium carbonate (2.00 mmol, 274 mg) in 7 mL of dimethoxyethane and 3.5 mL of distilled water is degassed with nitrogen for 20 min, and then tetrakis(triphenylphosphine)palladium (20 μ mol, 22 mg) is added. The reaction is heated to reflux temperature for 16 h. After cooling to room temperature, dichloromethane, water, and an oversaturated solution of Na₂SO₃ are added. The aqueous layer is extracted several times with small amounts of dichloromethane. The combined organic layers are dried with anhydrous sodium sulfate, and the solvent is removed *in vacuo*. The residue is chromatographed on silica gel (*n*-hexane/acetone 30:1) to give **2j** (123 mg, 83%) as a yellow solid, mp 217 °C. ¹H NMR (500 MHz, CD₂Cl₂): δ 0.92 (t, $J = 7$ Hz, 6 H), 1.37–1.39 (m, 8 H), 1.52–1.54 (m, 4 H), 1.90–1.96 (m, 4 H), 3.98 (t, $J = 7.0$ Hz, 4 H), 6.95–6.99 (m, 4 H), 7.11 (dd, $J = 2.5$ Hz, $J = 8.5$ Hz, 2 H), 7.16 (d, $J = 8$ Hz, 2 H), 7.21–7.24 (m, 6 H), 7.31–7.33 (m, 4 H), 7.73–7.75 (m, 4 H). ¹³C NMR (125 MHz, CD₂Cl₂): δ 14.1 (CH₃), 23.0 (CH₂), 27.0 (CH₂), 27.2 (CH₂), 31.9 (CH₂), 47.9 (CH₂), 115.61 (CH), 115.66 (CH), 115.9 (CH), 122.7 (CH), 124.9 (C_{quat}), 125.11 (C_{quat}), 125.15 (C_{quat}), 125.3 (CH), 127.2 (CH), 127.7 (CH), 130.15 (CH), 130.19 (CH), 130.4 (C_{quat}), 130.61 (CH), 130.66 (CH), 133.2 (C_{quat}), 136.5 (C_{quat}), 145.1 (C_{quat}), 145.6 (C_{quat}). MALDI MS $m/z = 740.3$ (EM = 740.325). UV-vis (CH₂Cl₂): λ_{\max} (ϵ) = 258 nm (109200), 315 nm (13000), 359 nm (10900), 379 nm (15800), 398 nm (17000). IR (KBr): $\tilde{\nu} = 2927$ cm⁻¹, 1543, 1498, 1465, 770, 749. Anal. Calcd for C₅₀H₄₈N₂S₂ (741.6): C 81.04, H 6.53, N 3.78. Found: C 80.93, H 6.67, N, 3.59.

3,9-(10)-Bis(10-hexyl-10*H*-phenothiazin-3-yl)perylene (2k). A mixture of 3,9(10)-dibromoperylene (**4c**) (0.18 mmol, 77 mg),

(32) *Organikum*, 21st ed.; Becker, H. G. O.; Beckert, R.; Domschke, G.; Fanghanel, E.; Habicher, W. D.; Metz, P.; Pavel, D.; Schwetlick, K. Wiley-VCH: Weinheim, New York, Chichester, Brisbane, Singapore, Toronto, 2001.

(33) Miller, L. L.; Yu, Y. *J. Org. Chem.* **1995**, *60*, 6813–6819.

(34) Sonnenschein, M.; Amirav, A.; Jortner, J. *J. Phys. Chem.* **1984**, *88*, 4218–4222.

(35) Nad, S.; Pal, H. *J. Phys. Chem. A* **2001**, *105*, 1097–1106.

(36) Melhuish, H. *J. Phys. Chem.* **1961**, *65*, 229–235.

(37) Jones, G. II; Rahman, M. A. *J. Phys. Chem.* **1994**, *98*, 13028–13037.

(38) Hamai, S.; Hirayama, F. *J. Phys. Chem.* **1983**, *87*, 83–89.

(39) Zanello, P. In *Ferrocenes*; Togni, A.; Hayashi, T., Eds.; VCH: Weinheim, New York, Basel, Cambridge, Tokyo, 1995; pp 317–430.

10-hexyl-10*H*-phenothiazin-3-yl pinacolyl boronic ester (**3**) (0.34 mmol, 140 mg), and potassium carbonate (1.70 mmol, 236 mg) in 6 mL of dimethoxyethane and 3 mL of distilled water is degassed with nitrogen for 20 min before the catalyst tetrakis[triphenylphosphine]palladium (17 μ mol, 196 mg) is added. The reaction is heated to reflux temperature for 7 h. After cooling to room temperature, dichloromethane, water, and an oversaturated solution of Na₂SO₃ are added. The aqueous layer is extracted several times with small amounts of dichloromethane. The combined organic layers are dried with anhydrous sodium sulfate, and the solvent is removed *in vacuo*. The residue is chromatographed on silica gel (*n*-hexane/acetone 10:1) to give **2k** (95 mg, 67%) as an orange solid, mp 199–200 °C. ¹H NMR (500 MHz, CD₂Cl₂): δ 0.86 (t, *J* = 7.0 Hz, 6 H), 1.32–1.33 (m, 8 H), 1.44–1.47 (m, 4 H), 1.82–1.88 (m, 4 H), 3.91 (t, *J* = 7.0 Hz, 4 H), 6.91–6.94 (m, 4 H), 7.00 (d, *J* = 8.0 Hz, 2 H), 7.14 (dd, *J* = 8.0 Hz, *J* = 1.5 Hz, 2 H), 7.18 (td, *J* = 6.8 Hz, *J* = 1.5 Hz, 2 H), 7.28 (d, *J* = 2.0 Hz, 2 H), 7.30 (dd, *J* = 8.5 Hz, *J* = 2.0 Hz, 2 H), 7.40 (d, *J* = 7.5 Hz, 2 H), 7.44 (t, *J* = 8.0 Hz, 2 H), 7.79 (dd, *J* = 8.5 Hz, *J* = 2.0 Hz, 2 H), 8.23 (d, *J* = 7.5 Hz, 4 H). ¹³C NMR (125 MHz, CD₂Cl₂): δ 14.2 (CH₃), 23.4 (CH₂), 27.4 (CH₂), 27.7 (CH₂), 32.3 (CH₂), 47.9 (CH₂), 116.0 (CH), 116.3 (CH), 120.7 (CH), 120.9 (CH), 121.1 (CH), 121.3 (CH), 123.0 (CH), 125.5 (C_{quat}), 125.8 (C_{quat}), 126.52 (CH), 126.59 (CH), 127.3 (CH), 127.95 (CH), 127.98 (CH), 128.3 (CH), 129.1 (CH), 129.5 (CH), 129.7 (C_{quat}), 131.3 (C_{quat}), 131.4 (C_{quat}), 132.2 (C_{quat}), 132.4 (C_{quat}), 133.7 (C_{quat}), 135.7 (C_{quat}), 139.7 (C_{quat}), 139.8 (C_{quat}), 145.6 (C_{quat}), 146.0 (C_{quat}). UV–vis (CH₂Cl₂): λ_{\max} (ϵ) = 259 nm (117000), 316 nm (11100), 441 nm (32500), 468 nm (60300). IR (KBr): $\tilde{\nu}$ = 2924 cm⁻¹, 1577, 1560, 1543, 1523, 1508, 1491, 746. MALDI MS *m/z* = 814.3 (EM = 814.34). Anal. Calcd for C₅₆H₅₀N₂S₂ (815.1): C 82.51, H 6.18, N 3.44. Found: C 82.41, H 6.33, N 3.26.

3,6-Bis(10-hexyl-10*H*-phenothiazin-3-yl)-pyridazine (2l). A mixture of 3,6-dibromo-pyridazine (**4d**) (0.195 mmol, 46 mg), 10-hexyl-10*H*-phenothiazin-3-yl pinacolyl boronic ester (**3**) (0.43 mmol, 176 mg), and potassium carbonate (1.95 mmol, 269 mg) in a mixture of 8 mL of dimethoxyethane and 4 mL of distilled water is degassed with nitrogen for 20 min, and then tetrakis[triphenylphosphine]palladium (19 μ mol, 22 mg) is added. The reaction is heated to reflux temperature overnight. After cooling to room temperature, dichloromethane, water, and an oversaturated solution of Na₂SO₃ are added. The aqueous layer is extracted several times with small amounts of dichloromethane. The combined organic layers are dried with anhydrous sodium sulfate and the solvent is removed *in vacuo*. The residue is chromatographed on silica gel (*n*-hexane/acetone 10:1) to give **2l** (92 mg, 74%) as a yellow solid, mp 104–105 °C. ¹H NMR (500 MHz, CD₂Cl₂): δ 0.88 (t, *J* = 7.1 Hz, 6 H), 1.28–1.37 (m, 8 H), 1.43–1.51 (m, 4 H), 1.77–1.90 (m, 4 H), 3.91 (t, *J* = 7.2 Hz, 4 H), 6.90–6.98 (m, 4 H), 7.01 (d, *J* = 8.6 Hz, 2 H), 7.12–7.22 (m, 4 H), 7.81 (s, 2 H), 7.90 (d, *J* = 2.1 Hz, 2 H), 7.96 (dd, *J* = 8.5 Hz, *J* = 2.2 Hz, 2 H). ¹³C NMR (125 MHz, CD₂Cl₂): δ 14.1 (CH₃), 22.9 (CH₂), 26.9 (CH₂), 27.1 (CH₂), 31.8 (CH₂), 47.9 (CH₂), 115.8 (CH), 115.9 (CH), 123.0 (CH), 123.4 (CH), 124.3 (C_{quat}), 125.4 (C_{quat}), 125.5 (CH), 126.1 (CH), 127.6 (CH), 127.7 (CH), 130.5 (C_{quat}), 144.9 (C_{quat}), 147.1 (C_{quat}), 156.3 (C_{quat}). MALDI MS: *m/z* = 642.2 (EM = 642.29). UV–vis (CH₂Cl₂): λ_{\max} (ϵ) = 278 nm (40500), 299 (34300), 394 nm (26300). IR (KBr): $\tilde{\nu}$ = 2926 cm⁻¹, 1637, 1577, 1560, 1543, 1499, 1458, 747. Anal. Calcd for C₄₀H₄₂N₄S₂ (642.9): C 74.73, H 6.58, N 8.71. Found: C 74.78, H 6.82, N 8.56.

2,5-Bis[10-hexyl-10*H*-phenothiazin-3-yl]thiophene (2m). In a Schlenk flask 2,5-diiodo thiophene (**4e**) (150 mg, 0.45 mmol), 10-hexyl-10*H*-phenothiazin-3-yl pinacolyl boronic ester (**3**) (0.94 mmol, 384 mg), and NaHCO₃ (2.68 mmol, 225 mg) dissolved in a mixture of DME (7 mL) and H₂O (3 mL) are degassed in a stream of nitrogen for 10 min. Then Pd(PPh₃)₄ (27 μ mol, 31 mg)

is added, and the reaction mixture is heated to reflux temperature for 12 h. After cooling to room temperature, the reaction is extracted with diethyl ether (50 mL), and the ethereal extracts are washed twice with water. After drying of the organic layers with anhydrous magnesium sulfate, the solvents are removed *in vacuo*. The residue is purified by column chromatography on silica (diethyl ether/pentane 1:25) to give **2m** (222 mg, 77%) as a yellow resin, *R_f*(diethyl ether/pentane) (1:25) = 0.19. ¹H NMR (CD₂Cl₂, 300 MHz): δ 0.79 (m_c, 6 H), 1.18–1.24 (m, 8 H), 1.35 (m_c, 4 H), 1.71 (m_c, 4H), 3.77 (t, *J* = 7.0 Hz, 4 H), 6.76–6.85 (m, 6 H), 7.03–7.11 (m, 6 H), 7.27–7.32 (m, 4 H). ¹³C NMR (CD₂Cl₂, 75 MHz): δ 13.8 (CH₃), 22.7 (CH₂), 26.6 (CH₂), 26.9 (CH₂), 31.5 (CH₂), 47.6 (CH₂), 115.5 (CH), 115.6 (CH), 122.5 (CH), 123.2 (CH), 124.0 (CH), 124.1 (C_{quat}), 124.5 (CH), 125.3 (C_{quat}), 127.3 (CH), 127.4 (CH), 128.7 (C_{quat}), 141.9 (C_{quat}), 144.6 (C_{quat}), 145.0 (C_{quat}). MS (EI+, 70 eV) *m/z* (%): 648 (16), 647 (37), 646 (M⁺, 100), 562 (10), 561 (21), 476 (21). IR (KBr): $\tilde{\nu}$ = 2925 cm⁻¹, 1461, 747. UV–vis (CHCl₃): λ_{\max} (ϵ) = 245 nm (33000), 258 nm (32300), 321 nm (21700), 390 nm (26000). Anal. Calcd for C₄₀H₄₂N₂S₃ (646.9): C 74.26, H 6.54, N 4.33, S 14.87. Found: C 74.28, H 6.58, N 4.11, S 14.71.

5,5'-Di-10-*n*-hexyl-10*H*-phenothiazin-[2,2']-bithiophene (2n). In a Schlenk flask 5,5'-diiodo-[2,2']-bithiophene (**4f**) (211 mg, 0.50 mmol), 10-hexyl-10*H*-phenothiazin-3-yl pinacolyl boronic ester (**3**) (409 mg, 1.00 mmol), and K₂CO₃ (276 mg, 2.00 mmol) dissolved in a mixture of DME (50 mL) and H₂O (25 mL) are degassed in a stream of nitrogen for 10 min. Then Pd(PPh₃)₄ (23 μ mol, 26 mg) is added, and the reaction mixture is heated to reflux temperature for 48 h. After cooling to room temperature, water is added, and the aqueous phase is extracted with dichloromethane (3 \times 50 mL). After drying of the organic layers with anhydrous magnesium sulfate, the solvents are removed *in vacuo*. Upon concentration the product precipitates and is collected by suction to give **2n** (280 mg, 70%) as a shiny orange solid, mp 146–148 °C. ¹H NMR (300 MHz, CD₂Cl₂): δ 0.88 (m, 6 H), 1.26–1.34 (m, 8 H), 1.44 (m_c, 4 H), 1.80 (m_c, 4 H), 3.85 (t, *J* = 7.2 Hz, 4 H), 6.87 (m, 4 H), 6.93 (m, 2 H), 7.1 (m, 6 H), 7.16 (m, 2 H), 7.35 (d, *J* = 1.9 Hz, 2 H), 7.38 (dd, *J* = 8.3 Hz, *J* = 2.2 Hz, 2 H). ¹³C NMR (75 MHz, CD₂Cl₂): δ 14.1 (CH₃), 22.9 (CH₂), 26.9 (CH₂), 27.1 (CH₂), 31.8 (CH₂), 47.8 (CH₂), 115.8 (CH), 115.9 (CH), 122.8 (CH), 123.3 (CH), 124.30 (CH), 124.31 (C_{quat}), 124.7 (CH), 124.8 (CH), 125.7 (C_{quat}), 127.6 (CH), 127.7 (CH), 128.7 (C_{quat}), 136.2 (C_{quat}), 142.4 (C_{quat}), 145.1 (C_{quat}), 145.2 (C_{quat}). FAB⁺ MS *m/z* (%): 728 ([M – H]⁺, 6), 307 ([M – PT – C₂HS]⁺, 100). UV–vis (CH₂Cl₂): λ_{\max} (ϵ) 250 nm (38300), 266 nm (37300), 338 nm (17800), 418 nm (4400). IR (KBr): $\tilde{\nu}$ = 3061 cm⁻¹, 1491, 1471, 1442, 1433, 1365, 1251, 1244, 798, 750. Anal. Calcd for C₄₄H₄₄N₂S₄ (729.1): C 72.48, H 6.08, N 3.84. Found: C 72.18, H 6.12, N 3.84.

7,7'-(Anthracene-9,10-diyl)bis(10-hexyl-10*H*-phenothiazine-3-carbonitrile (2o). A mixture of 9,10-di(4,4,5,5-tetramethyl-1,3,2-dioxaborolan-2-yl)anthracene (**5**) (0.307 mmol, 0.132 g), 3-bromo-7-cyano-10-hexyl-10*H*-phenothiazine (**7**) (0.676 mmol, 0.262 g), and potassium carbonate (3.07 mmol, 423 mg) in a mixture of dimethoxyethane (3 mL) and distilled water (1.5 mL) is degassed with nitrogen for 20 min, and then tetrakis[triphenylphosphine]palladium (30 μ mol, 35 mg) is added. The reaction mixture was heated to reflux temperature for 9 h. After cooling to room temperature, dichloromethane, water, and an oversaturated solution of Na₂SO₃ are added. The aqueous layer is extracted several times with small amounts of dichloromethane. The combined organic layers are dried with anhydrous sodium sulfate, and the solvent is removed *in vacuo*. The residue is chromatographed on silica gel (hexane/acetone 20:1) to give **2o** (125 mg, 51%) as a yellow solid, mp 294 °C. ¹H NMR (500 MHz, CD₂Cl₂): δ 0.92 (t, *J* = 7 Hz, 6 H), 1.37–1.40 (m, 8 H), 1.51–1.56 (m, 4 H), 1.89–1.95 (m, 4 H), 3.99 (t, *J* = 7.75 Hz, 4 H), 6.96 (d, *J* = 8.5 Hz, 2 H), 7.12–7.14 (m, 2 H), 7.18–7.20 (m, 2 H),

7.23–7.27 (m, 2 H), 7.33–7.37 (m, 6 H), 7.48–7.50 (m, 2 H), 7.71–7.73 (m, 4 H). ^{13}C NMR (125 MHz, CD_2Cl_2): δ 14.1 (CH_3), 22.9 (CH_2), 26.8 (CH_2), 26.9 (CH_2), 31.7 (CH_2), 48.3 (CH_2), 105.5 (C_{quat}), 115.6 (CH), 116.26 (CH), 116.29 (CH), 119.0 (C_{quat}), 123.7 (C_{quat}), 123.8 (C_{quat}), 125.5 (CH), 127.0 (CH), 130.2 (CH), 130.3 (CH), 130.6 (CH), 131.0 (CH), 131.1 (CH), 132.2 (CH), 134.5 (C_{quat}), 136.1 (C_{quat}), 143.4 (C_{quat}), 149.5 (C_{quat}). MALDI MS m/z = 790.286 (EM = 790.32). UV-vis (CH_2Cl_2): λ_{max} (ϵ) = 259 nm (115400), 266 nm (116000), 327 nm (12600), 341 nm (13800), 360 nm (10900), 379 nm (21400), 398 nm (21800). IR (KBr): $\tilde{\nu}$ = 2928 cm^{-1} , 2223, 1468, 1388, 1246, 1198, 769. Anal. Calcd for $\text{C}_{52}\text{H}_{46}\text{N}_4\text{S}_2$ (791.1): C 78.95, H 5.86, N 7.08. Found: C 78.67, H 6.16, N, 7.11.

3-(Anthracen-9-yl)-10-hexyl-10H-phenothiazine (9). A mixture of 9-bromoanthracene (0.80 mmol, 207 mg), 10-hexyl-10H-phenothiazin-3-yl pinacolyl boronic ester (**3**) (0.73 mmol, 301 mg), and potassium carbonate (5.14 mmol, 710 mg) in a mixture of dimethoxyethane (8 mL) and distilled water (4 mL) is degassed with nitrogen for 20 min, and then tetrakis[triphenylphosphine]palladium (36 μmol , 42 mg) is added. The reaction mixture was heated to reflux temperature for 16 h. After cooling to room temperature, dichloromethane, water, and an oversaturated solution of Na_2SO_3 are added. The aqueous layer is extracted several times with small amounts of dichloromethane. The combined organic layers are dried with anhydrous sodium sulfate, and the solvent is removed *in vacuo*. The residue is chromatographed on silica gel (*n*-hexane/acetone 40:1) to give **9** (194 mg, 60%) as a yellow solid, mp 87 °C. ^1H NMR (500 MHz, CD_2Cl_2): δ 0.91 (t, J = 6.75 Hz, 3 H), 1.34–1.39 (m, 4 H), 1.49–1.54 (m, 2 H), 1.88–1.94 (m, 2 H), 3.97 (t, J = 6.75 Hz, 2 H),

6.94–6.99 (m, 2 H), 7.09 (d, J = 8 Hz, 1 H), 7.15–7.24 (m, 4 H), 7.34–7.37 (m, 2 H), 7.46 (t, J = 7.5 Hz, 2 H), 7.72 (d, J = 9 Hz, 2 H), 8.04 (d, J = 8.5 Hz, 2 H), 8.49 (s, 1 H). ^{13}C NMR (125 MHz, CD_2Cl_2): δ 14.1 (CH_3), 23.0 (CH_2), 27.0 (CH_2), 27.2 (CH_2), 31.8 (CH_2), 47.8 (CH_2), 115.5 (CH), 115.8 (CH), 122.7 (CH), 124.8 (C_{quat}), 125.0 (C_{quat}), 125.4 (CH), 125.6 (CH), 126.7 (CH), 127.0 (CH), 127.7 (CH), 128.5 (CH), 130.0 (CH), 130.5 (CH), 130.6 (C_{quat}), 131.7 (C_{quat}), 132.9 (C_{quat}), 136.4 (C_{quat}), 145.1 (C_{quat}), 145.6 (C_{quat}). MALDI MS m/z = 459.1. UV-vis (CH_2Cl_2): λ_{max} (ϵ) = 255 nm (14200), 317 nm (7000), 332 nm (7000), 350 nm (8300), 368 nm (11100), 388 nm (11000). IR (KBr): $\tilde{\nu}$ = 2926 cm^{-1} , 1464, 1358, 1251, 886, 814, 737. Anal. Calcd for $\text{C}_{32}\text{H}_{29}\text{NS}$ (459.6): C 83.62, H 6.36, N 3.05. Found: C 83.55; H 6.11; N 3.14.

Acknowledgment. The support of this work by the Deutsche Forschungsgemeinschaft DFG (Graduate College 850, stipend for K.M.), by the Deutscher Akademischer Austauschdienst DAAD (scholarship for R.T.), and by the Fonds der Chemischen Industrie is gratefully acknowledged. The authors also thank the BASF AG for the generous donation of chemicals.

Supporting Information Available: Selected spectra (^1H and ^{13}C NMR, UV-vis, and fluorescence spectra) and cyclovoltammetric data of compounds **2g–o** and **9**, crystallographic data of **2n**, and molecular modeling coordinates and FMO energies of **2g–o**. This material is available free of charge via the Internet at <http://pubs.acs.org>.